Extremely Slow Dynamics of a Weakly Wetting Liquid at a Solid/Liquid Interface: CS_2 Confined in Nanoporous Glasses

Brian J. Loughnane, Alessandra Scodinu, and John T. Fourkas*

Eugene F. Merkert Chemistry Center, Boston College, Chestnut Hill, Massachusetts 02467

Received: April 8, 1999; In Final Form: May 24, 1999

The orientational dynamics of liquid CS_2 confined in silicate nanopores have been studied over a broad range of temperatures using optical Kerr effect spectroscopy. The average orientational correlation time is found to depend strongly on the pore size. Improvements in dynamic range of the data compared to previous studies have revealed orientational relaxation that occurs more than an order of magnitude more slowly than in bulk CS_2, despite the lack of strong interactions between the liquid and the pore surfaces. By studying the pore size dependence of the relaxation, we are able to separate the contributions of energetics, hydrodynamic volume, and geometrical constraints to the retardation of dynamics at the pore surfaces.

I. Introduction

Understanding the behavior of liquids at liquid/solid interfaces is of great relevance to a broad range of scientific problems.[1−5] The structural and dynamic details of weakly wetting liquids at such interfaces are of particular significance to important technological areas such as lubrication, which has spurred a considerable amount of theoretical[6−14] and experimental[15−26] work in this area.

A daunting challenge in studying such systems is that it can be difficult to isolate the behavior of interfacial liquid molecules from that of the considerably more abundant bulk liquid molecules. One general approach that has been used successfully to address this problem is to reduce the fraction of bulk liquid molecules substantially and in a controlled manner. For example, surface-force apparatus experiments have proven to be a powerful means of exploring the structure, collective dynamics, and mechanical properties of weakly wetting liquids confined between two parallel, atomically flat solid surfaces separated by a small distance.[15,17,25,26]

Confinement of weakly wetting liquids in nanoporous media, which have extremely high surface-to-volume ratios, is another useful means of effecting a considerable reduction in the fraction of bulk liquid so that the behavior of the interfacial population of liquid molecules can be probed. Porous silicate glasses have proven to be particularly useful materials in this regard. Using sol−gel technology, glass samples can be prepared with a narrow distribution of pores sizes centered about a controllable average pore size.[27] These materials are relatively pure and have good optical quality and so are amenable to use with a wide range of experimental techniques. For instance, the dynamics of weakly wetting liquids have been studied in these materials with techniques that include NMR spectroscopy,[28−35] Raman spectroscopy,[36−38] and optical Kerr effect (OKE) spectroscopy.[39−41]

Carbon disulfide has figured prominently in studies of weakly wetting liquids confined to nanoporous glasses. Indeed, this liquid was the subject of the first experiments designed to investigate molecular dynamics in these materials.[39] On the basis of this work, which employed OKE[42] spectroscopy, Warnock, Awschalom, and Schafer[39] concluded that the reorientational dynamics of CS_2 in confinement mirror those observed in the bulk liquid. More recent Raman spectroscopic studies by Wallen, Nikiel, and Jonas[38] revealed a measurable change in the orientational correlation time of CS_2 upon nanoconfinement, which was further supported by the NMR studies of Korb et al.[35] OKE experiments performed in our laboratory[40] demonstrated that the orientational correlation function of CS_2 confined to pores 24 Å in diameter is significantly nonexponential. We were able to fit the OKE data to the sum of two exponentials, one of which had a decay constant matching the orientational correlation time in the bulk liquid and the other of which was several times slower.[40] This latter exponential was interpreted as reflecting inhibited orientational dynamics of CS_2 molecules near the pore surfaces. The data also revealed that the population experiencing inhibited dynamics due to proximity to the pore surfaces comprised less than a single layer of CS_2 molecules.

Here we present the results of a considerably more detailed temperature-dependent OKE study of the dynamics of CS_2 confined in sol−gel glasses than we have presented previously.[40] While our previous work concentrated on CS_2 dynamics in 24 Å pores, here we employ glasses with a range of average pore sizes, which allows us to separate the contributions of different mechanisms that lead to the retardation of the liquid dynamics near the pore surfaces. Improvements in our experimental apparatus have expanded the dynamic range of our OKE data significantly, which has allowed us to monitor the orientational correlation function over a much longer period of time than was possible previously. As a result, we have observed a new, extremely slow relaxation component in the OKE decays of confined CS_2.

II. Experimental Section

Monolithic nanoporous sol−gel glass samples were prepared as described elsewhere.[41] The pore size distribution for each sample was determined from Pierce adsorption isotherms[43,44] measured with a BET sorptmeter (PMI/APP). Samples with four different average pore diameters were employed: 21, 25, 28, and 45 Å. For optical studies, the cylindrical monoliths, which had diameters of approximately 6 mm, were ground to a thickness of 2 mm and then polished to optical quality using diamond paste. The polished monoliths were placed in a 2 mm path length quartz optical cell, one end of which was subsequently sealed. Before being filled with liquid, the cell was

10.1021/jp991176u CCC: $18.00
Published on Web 07/02/1999

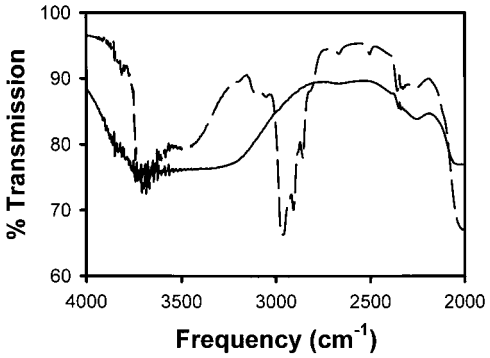

Figure 1. Infrared spectra of unmodified (solid line) and modified (dashed line) sol−gel glasses with an average pore size of 45 Å. Surface modification with chlorotrimethylsilane decreases considerably the band near 3800 cm^{-1} due to surface OH groups, as well as a band near 3400 cm^{-1} caused by a small amount of physisorbed water. The band near 3650 cm^{-1} in both samples arises from internal hydroxyl groups, and the band at 2900 cm^{-1} in the modified samples arises from the methyl groups of the trimethylsilane.

heated to 450 °C to remove any impurities that might have accumulated during the polishing or glass-blowing procedures.

Surface-modified samples were prepared by refluxing monoliths within an optical cell in a 50% solution of chlorotrimethylsilane in toluene for a period of at least 96 h. The samples were then washed successively in toluene, benzene, and methanol, after which they were placed in a 100 °C vacuum oven for 24 h to remove any remaining volatile adsorbates. The extent of the surface modification was later verified by infrared spectroscopy. Typical spectra of unmodified and modified samples are shown in Figure 1. Surface hydroxyl groups lead to a prominent feature near 3800 cm^{-1}.[27,45,46] This band is not present in the IR spectrum of the modified sample, which indicates that the silanization procedure removed virtually 100% of the surface hydroxyl groups in the sol−gel samples. The decrease in the band near 3400 cm^{-1} upon surface modification arises from the removal of a small amount of water physisorbed on the pore surfaces, and the remaining band at 3650 cm^{-1} arises from internal hydroxyl groups (which are not accessible to any fluid confined in the pores).[45,46] Pierce adsorption isotherms obtained after surface modification revealed a slight decrease in average pore diameter, and decreased BET constants[44] indicated a significant decrease in the surface adsorption energy.

Carbon disulfide was distilled carefully and then filtered several times through 0.1 μm Millipore filters before being introduced into the sample cell. Enough liquid was added to immerse the monoliths completely, and then the cell was sealed and mounted on a brass sample holder in a continuous-flow vacuum cryostat (Janis ST-100). A silicon diode probe was placed directly on the surface of the sample cell to obtain accurate temperature readings.

As mentioned above, the dynamic range of our OKE apparatus has been enhanced considerably since our initial experiments on confined CS_2.[40] The improved apparatus has been described thoroughly in a recent publication,[41] and the experimental details are essentially identical in the present study of CS_2. We will therefore discuss only those details that are unique to the current experiments.

To study diffusive reorientation, OKE scans were obtained with time steps of 133 fs out to the maximum delay for which useful data could be recorded. To study intermolecular dynamics, data with a time step of 6.67 fs were recorded out to a delay time of 10 ps. A tail with the same step size was stripped onto these data based on fits of the long-step reorientation data.

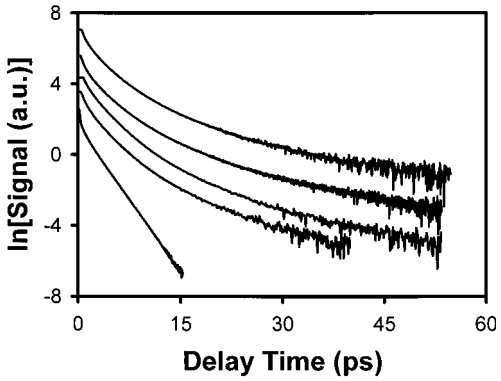

Figure 2. Representative CS_2 OKE scans obtained at 290 K. The scans, from bottom to top, are in the bulk liquid and in confinement in 45, 28, 25, and 21 Å pores.

The concatenated short-step data, in conjunction with second harmonic autocorrelation data, were subjected to the Fourier transform deconvolution procedure of McMorrow and Lotshaw[47] to compute the Bose−Einstein corrected Rayleigh-wing spectrum.[48] The corresponding nuclear response function was calculated by performing an inverse Fourier transform of the spectrum. The orientational diffusion portion of the nuclear response function was then removed using an assumed rise time of 150 fs to generate the intermolecular nuclear response function, which is the negative time derivative of the intermolecular polarizability correlation function (PCF).[49] Because the tail of the intermolecular nuclear response function is exponential for CS_2, it is straightforward to find the appropriate constant of integration for converting the nuclear response function into the PCF.

III. Results

Representative CS_2 OKE data obtained at 290 K in the bulk liquid and in confinement in the various pore sizes are shown in Figure 2. In our previous study of this liquid confined in 24 Å pores, we found that after the first couple of picoseconds (in which intermolecular dynamics contribute to the OKE signal) the decays could be fit well by the sum of two exponentials.[40] The faster exponential had a time constant that matched that of the bulk liquid, whereas the slower exponential had a time constant that was several times larger. With the improved dynamic range of our apparatus, we are now able to monitor the OKE decays in this liquid over a considerably longer time range. While our new data are consistent with the previous data when viewed over the same limited range of delay times employed previously, when the full temporal range now available is considered a biexponential fit no longer provides an adequate description of the decays.

We have explored a number of different functions for fitting the new CS_2 data. For instance, when multiple time scales are involved in the relaxation dynamics of a system, the time dependence of the data can often be described by a stretched exponential, $\exp(-t/\tau)^{\beta}$, where τ is the characteristic relaxation time and β can range between 0 and 1. However, our data cannot be fit well by a stretched exponential. Similarly, the data cannot be described well by a power law decay or by the sum of a power law and an exponential. The data can be fit reasonably well by the sum of an exponential and a stretched exponential (a five-parameter model), and can be fit quite well by the sum of three exponentials (a six-parameter model). In both of the latter cases, the fastest exponential has a time constant (which we will denote τ_1) that is nearly identical to that for the OKE

decay in the bulk liquid. While we cannot ascribe direct physical significance to the functional form of the remaining portion of the decays, the same type of information can be extracted from any good fit of the long-time portion of the data, and so the exact model employed is not crucial to our analysis. In what follows, we will employ the results of the triexponential model, since it provides the most accurate description of the data and is convenient to work with.

For the triexponential fit, the decay time of the middle exponential (τ_2) is generally a factor of approximately 3 to 4 larger than that of the bulk liquid, which is consistent with our previous results in 24 Å pores.[40] The third exponential has a time constant (τ_3) that is approximately 3 to 4 times larger than that of the second exponential. That the time constant of the fastest exponential matches that of bulk CS_2 is consistent with our previous data in CS_2[40] and in methyl iodide.[41] This result suggests that weakly wetting liquids in confinement partition into at least two distinct populations, one whose orientational dynamics are bulklike and the other whose orientational dynamics are significantly retarded by proximity to the pore surfaces.

The decay parameters cannot be determined with a high degree of accuracy from completely unconstrained triexponential fits to the data. To improve the fits, we first constrained the time constant of the fastest exponential to match that of the bulk liquid and refit the data to find the second and third time constants. For each pore size, we then calculated an "effective viscosity"[40,41,50] for each surface exponential using (vide infra)

$$\eta_{\mathrm{eff},j} = \frac{\tau_j}{\tau_{\mathrm{bulk}}}\eta_{\mathrm{bulk}} \tag{1}$$

where $j = 2$ or 3. As we have found for other liquids,[41,50] the effective viscosity for each exponential in a given pore size obeys the Arrhenius equation. Least-squares Arrhenius fits were used to refine the time constants of each exponential in each pore size, and the decays were fit one last time to determine the amplitude A_j of each exponential. The final fitting parameters are listed in Table 1.

As we have discussed previously,[40] if the orientational correlation function of the confined liquid consists of a sum of exponentials, then the OKE signal will be given by

$$S(\tau) \propto \sum_j \frac{p_j}{\tau_j} \mathrm{e}^{-t/\tau_j} \tag{2}$$

where p_j is the fractional population of molecules that relax with the time constant τ_j. In such a case, the relative populations can therefore be calculated from the amplitudes and decay times of the exponentials. For the current data it is not clear whether the surface exponentials provide anything more than an empirical description of the retarded dynamics, so we must view the use of eq 2 as providing only an estimate of the relative populations.

Since it is not clear that τ_2 and τ_3 have direct physical relevance, for the purpose of analyzing the surface dynamics we will calculate a population-weighted average relaxation time for this population of molecules from the equation

$$\langle\tau_{\mathrm{surf}}\rangle = \frac{1}{p_{\mathrm{surf}}}(p_2\tau_2 + p_3\tau_3) \tag{3}$$

where $p_{\mathrm{surf}} = p_2 + p_3$. Similarly, we will calculate a total population-weighted average relaxation time using

TABLE 1: Reorientation Times and Amplitudes for Triexponential Fits[a]

T (K)	pore diameter (Å)	$\%A_1$	τ_1	$\%A_2$	τ_2	$\%A_3$	τ_3
165	21	73.0	13.02	24.3	45.8	2.9	214
	25	74.5	13.02	22.2	45.2	3.3	197
	28	75.7	13.02	21.8	35.9	2.5	143
	45	77.7	13.02	19.1	28.6	3.1	78.3
174	21	77.8	9.91	19.9	33.8	2.4	154
	25	72.6	9.91	25.0	33.3	2.4	141
	28	76.2	9.91	22.1	26.8	1.8	103
	45	78.6	9.91	18.1	22.1	3.3	60.6
194	21	75.5	6.48	21.9	19.7	2.6	85.4
	25	74.9	6.48	22.6	19.3	2.4	78.0
	28	78.1	6.48	19.7	15.9	2.1	58.2
	45	82.0	6.48	15.4	13.3	2.6	36.7
217	21	82.9	4.38	15.9	12.7	1.2	52.5
	25	77.6	4.38	20.9	12.3	1.5	47.7
	28	82.5	4.38	16.4	10.4	1.2	36.3
	45	83.5	4.38	15.1	8.8	1.4	24.5
254	21	77.7	2.68	21.5	7.3	0.8	28.7
	25	81.3	2.68	17.7	7.0	1.0	25.9
	28	82.1	2.68	17.2	6.2	0.7	20.1
	45	85.2	2.68	14.1	5.3	0.7	14.9
272	21	79.5	2.18	19.7	5.7	0.7	21.9
	25	79.9	2.18	19.2	5.5	0.9	19.7
	28	87.2	2.18	12.2	5.3	0.6	15.5
	45	86.8	2.18	12.6	4.3	0.6	12.1
290	21	80.1	1.84	19.2	4.6	0.7	17.4
	25	77.4	1.84	21.8	4.4	0.8	15.3
	28	89.5	1.84	10.1	4.3	0.5	12.2
	45	87.1	1.84	12.3	3.6	0.5	10.0
293	21	83.3	1.79	16.0	4.6	0.7	17.0
	25	78.3	1.79	20.9	4.4	0.8	15.3
	28	90.7	1.79	9.0	4.3	0.4	12.2
	45	89.1	1.79	10.5	3.5	0.4	9.9
310	21	84.7	1.55	14.9	3.9	0.4	14.5
	25	82.1	1.55	17.4	3.7	0.6	13.0
	28	91.4	1.55	8.3	3.8	0.3	10.3
	45	90.7	1.55	8.9	3.1	0.4	8.7

[a] All times are in picoseconds. Approximate uncertainties are 0.05 ps for τ_1 and 10% of the values for τ_2, τ_3, and the amplitude ratios. Note that the bulk decay times differ slightly from those we have reported previously[40] due to a temperature miscalibration in the original data.

$$\langle\tau\rangle = p_1\tau_1 + p_2\tau_2 + p_3\tau_3 \tag{4}$$

The values of $\langle\tau\rangle$, $\langle\tau_{\mathrm{surf}}\rangle$, and p_{surf} for each pore size are listed in Table 2.

IV. Discussion

Despite the fact that CS_2 is only weakly wetting on silicate glass, the data in Tables 1 and 2 reveal that a notable fraction of the confined molecules exhibit significant inhibition of reorientation. Indeed, the most striking feature of the data presented here is that in the smallest pores there is a relaxation component whose characteristic time scale for reorientation is more than an order of magnitude longer than that for the bulk liquid. This result is quite surprising in view of the lack of strong interactions between the liquid and the pore surfaces. Even in the largest pores studied, the third exponential decays considerably more slowly than does the signal in the bulk liquid. Furthermore, BET data show that there are no extremely narrow bottlenecks or micropores (i.e., pores with diameters of less than 20 Å) in the sample with a 45 Å average pore diameter, which strongly suggests that the retarded relaxation observed in confinement does indeed arise from molecules at the pore surfaces.

The orientational correlation time τ of a molecule in a simple liquid can be described by the Debye−Stokes−Einstein (DSE)

TABLE 2: Average Reorientation Times, Average Surface Reorientation Times, and Surface Populations[a]

T (K)	pore diameter (Å)	$\langle\tau\rangle$	$\langle\tau_{surf}\rangle$	p_{surf}
165	21	73.1	106	0.65
	25	71.6	106	0.63
	28	43.3	69.5	0.54
	45	26.7	44.1	0.44
174	21	47.7	75.9	0.57
	25	44.0	64.9	0.62
	28	27.7	44.9	0.51
	45	20.7	34.8	0.43
194	21	26.8	42.0	0.54
	25	23.6	37.0	0.56
	28	16.4	27.9	0.46
	45	11.6	20.6	0.36
217	21	11.9	22.2	0.48
	25	12.1	20.1	0.49
	28	8.56	15.6	0.37
	45	6.77	12.0	0.31
254	21	6.10	10.1	0.46
	25	5.79	10.3	0.45
	28	4.46	7.75	0.41
	45	3.74	6.55	0.27
272	21	4.55	7.75	0.43
	25	4.36	7.46	0.41
	28	3.38	6.51	0.28
	45	2.93	5.22	0.25
290	21	3.60	6.18	0.41
	25	3.50	5.69	0.43
	28	2.63	5.27	0.23
	45	2.41	4.27	0.24
293	21	3.38	6.19	0.36
	25	3.44	5.67	0.43
	28	2.48	5.09	0.21
	45	2.26	4.08	0.20
310	21	2.64	4.87	0.33
	25	2.68	4.68	0.36
	28	2.10	4.38	0.20
	45	1.93	3.68	0.18

[a] All times are in picoseconds. Approximate uncertainties 5% for $\langle\tau_{surf}\rangle$ and p_{surf}.

equation[51]

$$\tau = \frac{4\pi\eta r^3}{3k_B T} \tag{5}$$

where η is the viscosity, r is the hydrodynamic radius of the molecule, and k_B is Boltzmann's constant. An additional factor is often incorporated in this equation to account for whether the boundary conditions for reorientation are "stick" or "slip," i.e., whether the solute carries a layer of solvent along with it as it reorients. Although the DSE equation is not intended to be applicable to pure liquids, it is still generally found that the orientational correlation time is proportional to η/T even when the "solute" is identical to the solvent.[52]

One can imagine three factors in the DSE equation that might change at a solid/liquid interface: the viscosity, the hydrodynamic volume for reorientation, and the boundary condition for reorientation. The temperature dependence of τ can help to distinguish which of these factors affect surface reorientation in the system studied here, since of these parameters only the viscosity should depend significantly on temperature. Furthermore, it is generally the case that the viscosity of a simple liquid exhibits Arrhenius behavior. We have therefore employed eq 1 to calculate an effective surface viscosity using the bulk orientational time, the bulk viscosity, and $\langle\tau_{surf}\rangle$. We plot ln($\eta_{eff}$) versus $1/T$ in Figure 3, from which it can be seen that the effective viscosity does indeed adhere to the Arrhenius equation.

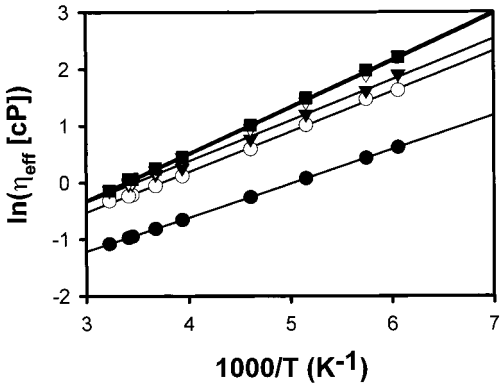

Figure 3. Arrhenius plots of the bulk viscosity (solid circles) and effective surface viscosities in 45 Å pores (open circles), 28 Å pores (solid triangles), 25 Å pores (open triangles), and 21 Å pores (solid squares).

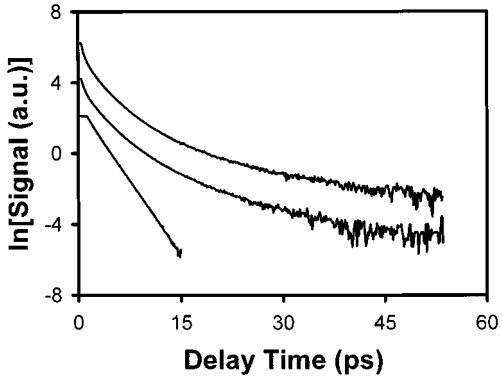

Figure 4. CS_2 OKE scans obtained at 293 K in, from bottom to top, the bulk liquid, 45 Å unmodified pores, and 45 Å modified pores. Note that the relaxation changes very little upon surface modification.

While the significant offset between the bulk and surface Arrhenius plots reaffirms the considerable difference in relaxation rates, perhaps the most striking feature in Figure 3 is that the activation energy implied by the effective surface viscosities in the pores is only slightly greater than that in the bulk liquid, with a trend toward a higher activation energy in smaller pores. The activation energy for the bulk liquid is 5.0 kJ/mol, compared to 5.9 kJ/mol for 45 Å pores, 6.0 kJ/mol for 28 Å pores, 6.8 kJ/mol for 25 Å pores, and 6.9 kJ/mol for 21 Å pores. We have previously suggested that surface hydroxyl groups or other sorts of surface "traps" could provide a possible explanation for the retardation of surface dynamics in this system. However, the fact that the activation energy for reorientation is not considerably greater at the pore surfaces than in the bulk argues against this explanation. Furthermore, surface modification with chlorotrimethylsilane should make hydroxyl groups or any other sort of surface trapping sites inaccessible to the confined liquid. However, as shown in Figure 4, modification of the pore surfaces in this manner leads to a slightly greater degree of retardation of surface dynamics. Taken together, these results show that energetics are not the primary source of the inhibition of reorientation of CS_2 at the pore surfaces, as we have also found for methyl iodide.[41] Thus, the true surface viscosity is considerably smaller than the effective viscosity that we have calculated, and conversely, whatever factors do contribute to the increased orientational correlation time at the pore surfaces are relatively insensitive to temperature.

It is also illuminating to consider the thickness of the layer of surface molecules that have inhibited dynamics. BET results

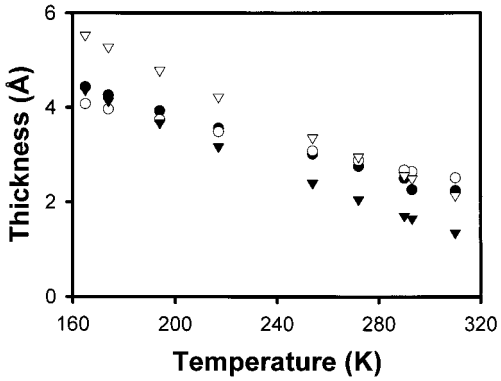

Figure 5. Estimated surface layer thickness in 21 Å pores (solid circles), 25 Å pores (open circles), 28 Å pores (solid triangles), and 45 Å pores (open triangles).

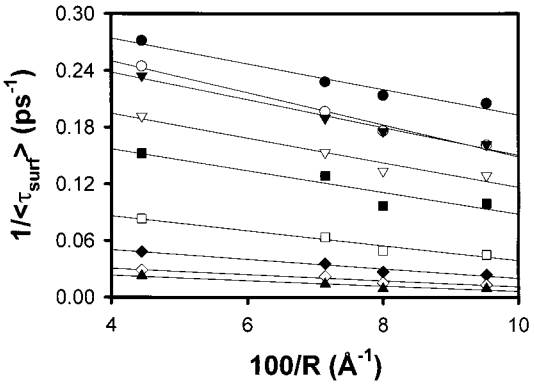

Figure 6. Surface reorientation rate versus pore curvature for, from bottom to top, 165, 174, 194, 271, 254, 272, 290, 293, and 310 K.

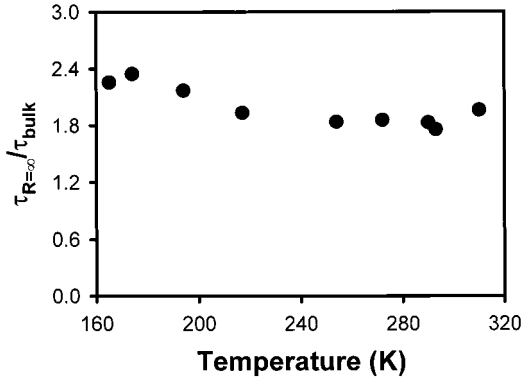

Figure 7. Ratio of the orientational correlation time at a flat surface to that in the bulk as a function of temperature. Within the experimental precision, the ratio is equal to the average value of 2.0 for all temperatures, which indicates that the hydrodynamic volume for CS_2 reorientation is twice as large at a flat surface as in the bulk liquid.

show that in all of our samples the pores are roughly cylindrical, so we can use the average pore radius in conjunction with p_{surf} to estimate the surface layer thickness. The results of such a calculation for each different pore size as a function of temperature are shown in Figure 5. The spread in the estimated thicknesses in different pore sizes at any given temperature is in the neighborhood of 1 Å, which probably reflects slightly different pore morphologies in the different samples. It is important to keep in mind that any deviation from cylindrical morphology will lead to an increased surface-to-volume ratio, so the data points in Figure 5 should be viewed as estimates of the maximum thickness that is consistent with the data for each pore size.

It is evident from Figure 5 that at the highest temperatures the surface layer thickness is appreciably less than the diameter of a single CS_2 molecule in its shortest dimension, 3.9 Å. At the lowest temperatures, the estimated surface layer thickness is comparable to the size of a single CS_2 molecule lying flat on the surface. Thus, over most of the liquid temperature range of CS_2, the population of molecules that displays retarded dynamics due to surface interactions appears to be less than one monolayer, as we have found previously for methyl iodide.[41]

Since the data in the surface-modified samples demonstrate that surface reorientation is inhibited even when no surface traps could exist, the fact that the surface layer can be less than one molecule thick suggests that the surface orientational correlation time of a given molecule may be influenced by the orientation of that molecule relative to the surface. We have already demonstrated that the retardation of surface dynamics is not due primarily to a change in viscosity, so we should examine in this light the other factors in the DSE equation that might change near a surface: the hydrodynamic volume and the boundary conditions for reorientation.

In the bulk liquid, a CS_2 molecule will reorient, on average, about its center of mass. The same will hold true for a surface CS_2 molecule whose long axis lies roughly along the surface normal. However, for a molecule lying flat on a surface to rotate off of the surface, the center of mass of the molecule must translate away from the surface. In other words, the hydrodynamic volume for the rotation of a molecule off of the surface must be greater than the hydrodynamic volume for rotation in the bulk liquid. That this effect comes into play only for molecules that sit roughly parallel to the surface explains why the thickness of the retarded surface layer can appear to be less than a monolayer. Furthermore, as the temperature is reduced, the degree of surface ordering should increase, which is consistent with the observed increase in the surface layer thickness.

Note that since the hydrodynamic volume effect arises for rotations about an axis that is parallel to the surface, it is not dependent on the curvature of the surface. We must consider different mechanisms for inhibition of reorientation about an axis normal to the pore surface. It is possible, for instance, that the effective friction for such reorientations is greater than that in the bulk liquid. However, in the system studied here, there are no strong interactions between liquid molecules or between the liquid and the pore surfaces, so we can expect slip conditions to apply in both cases. On the other hand, the boundary conditions for reorientation must still change at the pore surfaces due to geometric confinement effects; that is, in a curved pore, molecules at the surface are not free to reorient in a full three-dimensional space. This effect should be stronger in smaller, more highly curved pores, which is consistent with the $\langle\tau_{surf}\rangle$ data in Table 2. As in the case of the hydrodynamic volume, the reduced-dimensional effect will influence molecules that are lying parallel to the surface more strongly than those that lie closer to the surface normal.

Since geometrical confinement effects depend on the pore curvature while changes in hydrodynamic volume do not, we can distinguish the influences of these two mechanisms on surface reorientation. In particular, we can make an estimate of the orientational correlation time at a flat surface by considering its dependence on the pore size. In Figure 6, we plot the average rate of surface reorientation, $1/\langle\tau_{surf}\rangle$, versus the pore curvature. On the basis of these data, at each temperature we can make a linear extrapolation to estimate the orientational correlation time for an infinite radius of curvature, $\tau_{R=\infty}$. Figure 7 shows a plot of $\tau_{R=\infty}$ normalized to the bulk orientational correlation time as

a function of temperature. Within our experimental error, the value of $\tau_{R=\infty}/\tau$ is identical at all temperatures. The average value of the measurements is 2.0, which indicates that the hydrodynamic volume for reorientation of CS_2 doubles in going from the bulk liquid to a flat surface. Thus, the hydrodynamic volume effect is large enough to account for much of the increase in the orientational correlation time at the pore surfaces, particularly in larger pores. The appreciable pore size dependence to the surface orientational correlation time seen in Figure 7 demonstrates that geometrical confinement effects also play an important role, especially as the pore size decreases.

We should note that there exist a couple of other mechanisms that could increase the observed surface orientational correlation time. The first mechanism involves the potential densification of the confined liquid. It is well-known that liquids tend to have a greater degree of order near a solid surface than in the bulk, particularly in the presence of favorable surface solvation forces.[53−56] Ordered molecules can pack more tightly, and since the samples are immersed in CS_2, ordering of the molecules would lead to an overall increase in the density of the confined liquid as compared to the bulk liquid. A greater density would in turn lead to an increase in the viscosity of the confined liquid and a consequent retardation of dynamics. The moderate increase in the activation energy for reorientation at the surfaces relative to the bulk liquid seen in Figure 3 is consistent with this idea. On the other hand, the submonolayer thickness of the surface population suggests that the degree of surface ordering is not great enough to lead to any significant densification of the liquid in the pores as compared to the bulk. Additionally, since CS_2 wets the pore surfaces only weakly, the surface solvation forces should be fairly minimal. Finally, surface modification reduces any surface solvation forces even further, and so the fact that surface relaxation slows down slightly upon treatment of the pores with chlorotrimethylsilane therefore also argues against the importance of these forces in the observed dynamics.

It is also possible that the nature of the orientational relaxation observed in an OKE experiment can increase the apparent surface orientational correlation time. OKE spectroscopy measures the collective orientational correlation time, τ_c, rather than the single molecule orientational correlation time, τ_s. These two quantities are related by the equation

$$\tau_c = \frac{g_2}{j_2}\tau_s \tag{6}$$

where g_2 is the static orientational correlation parameter and j_2 is the dynamic orientational correlation parameter.[52] It is generally assumed that j_2 is approximately unity in simple liquids[52] so that the static orientational parameter accounts for any differences between τ_s and τ_c. The static orientational correlation parameter is given by

$$g_2 = 1 + n\frac{\langle P_2(1)P_2(2)\rangle}{\langle P_2(1)P_2(1)\rangle} \tag{7}$$

where n is the number density of the liquid, $P_2(i)$ is the second rank Legendre function of the orientation of molecule i, and the brackets indicate an average over all of the molecules in the liquid. The static orientational correlation parameter is usually greater than or equal to unity, so τ_c is always at least as large as τ_s. Comparison of values of τ_s derived from the ^{13}C NMR data of Korb et al.[35] with the data presented here suggests that g_2 has a value of approximately 1.5 for bulk CS_2. Since liquids do tend to order near surfaces, according to eq 7 the value of static orientational correlation parameter might be expected to be somewhat larger near the surfaces of pores. Furthermore, the magnitude of this effect would be expected to be sensitive to the size and morphology of a pore. Variations in g_2 between bulk and surface populations, as well as with pore size, may therefore complicate the analysis of the data presented here. For these reasons, it is particularly interesting to compare our results to those from NMR and Raman experiments on the same system, since these other techniques measure τ_s rather than the collective orientational correlation time.

Korb et al. have studied the temperature dependence of the ^{13}C and ^{33}S spin−lattice relaxation times for CS_2 in the bulk and confined in pores of various sizes.[35] The rate of spin−lattice relaxation in this system is the sum of the relaxation rates due to the spin−rotation interaction ($1/T_1^{SR}$) and the chemical shift anisotropy ($1/T_1^{CS}$). The relaxation rate for the spin−rotation interaction is given by

$$\frac{1}{T_1^{SR}} = \frac{4Ik_BTC_\perp^2}{3\hbar^2}\tau_J \tag{8}$$

where I is the moment of inertia of CS_2, $C_\perp$ is the spin-rotation constant, and τ_J is the angular momentum correlation time. The relaxation rate from the chemical shift anisotropy is given by

$$\frac{1}{T_1^{CS}} = \frac{2}{15}\omega^2(\Delta\sigma)^2\tau_s \tag{9}$$

where ω is the Larmor frequency and $\Delta\sigma$ is the chemical shift anisotropy of CS_2. Thus, in principle, the spin−lattice relaxation behavior of CS_2 can yield information about both single-molecule reorientational behavior and the angular momentum correlation time.

To separate the contributions of these two mechanisms to spin−lattice relaxation, Korb et al. studied the temperature dependence of T_1.[35] The spin−lattice relaxation time is highly sensitive to confinement. For instance, at 293 K it ranges from 42.9 s in the bulk liquid to 18.8 s in pores that are 102 Å in radius to 12.2 s in pores that are 15 Å in radius.[35] These results were analyzed with a model that assumes that reorientational motion parallel to the pore walls is unaffected by confinement, whereas reorientational motion perpendicular to the pore walls is inhibited. In comparison to a value of 1.21 ps for τ_s at 293 K in the bulk liquid, analysis with this model implied that the single molecule orientational correlation time increases by a factor of 1.1 (to 1.4 ps) in pores with a 102 Å radius and by a factor of 4.3 (to 5.2 ps) in pores with a 15 Å radius.[35] Similarly, τ_J was found to decrease from 95 fs in the bulk liquid to 40 fs in pores with a 102 Å radius and to 28 fs in pores with a 15 Å radius.[35]

We have found a value of 5.09 ps for $\langle\tau_{surf}\rangle$ and 2.48 ps for $\langle\tau\rangle$ in pores that are 14 Å in radius at 293 K. Surprisingly, the value of $\langle\tau\rangle$ we have measured is considerably smaller than the NMR value in a comparable pore size, and the value of $\langle\tau_{surf}\rangle$ is comparable to the NMR value of $\langle\tau\rangle$. The source of this discrepancy is not clear, but we are currently unable to combine the OKE and NMR data to extract g_2.

To further explore the relationship between the NMR and OKE data, we can investigate the Rayleigh-wing spectrum of CS_2. We have shown recently that the portion of the Rayleigh-wing spectrum of CS_2 that does not arise from orientational diffusion is dominated by scattering from the librational motions of single molecules (as opposed to scattering from a collision-

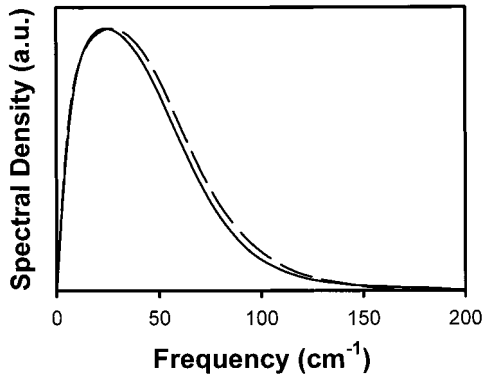

Figure 8. Bose−Einstein corrected Rayleigh-wing spectra for CS_2 in the bulk (solid line) and confined in 25 Å pores (dashed line). The reorientational component has been removed from both spectra. The resulting intermolecular spectra are identical to within the experimental accuracy.

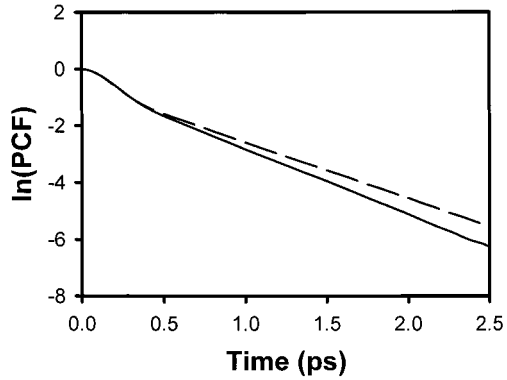

Figure 9. Intermolecular polarizability correlation functions for CS_2 in the bulk (solid line) and confined in 25 Å pores (dashed line).

induced mechanism).[57] The librational spectrum should therefore be strongly sensitive to changes in the angular momentum correlation time. We have used the Fourier transform deconvolution technique of McMorrow and Lotshaw[47] to calculate the Bose−Einstein corrected Rayleigh-wing spectrum of CS_2 from our OKE data. Rayleigh-wing spectra with the orientational diffusion contribution removed are illustrated in Figure 8 for CS_2 at 293 K in the bulk and confined in 25 Å pores. These spectra are practically identical to within the accuracy of the deconvolution procedure. For further comparison, we show the nondiffusive portion of the polarizability correlation function for the bulk and confined liquid in Figure 9. While these PCFs show slight deviations at long times, they are virtually identical for several hundred femtoseconds, which suggests that τ_J does not vary significantly from the bulk value even when the liquid is tightly confined.

Wallen et al. have used Raman spectroscopy to measure the average orientational correlation time of CS_2 in pores of various sizes at 293 K. They found a bulk orientational correlation time of 1.61 ps, which, when combined with the OKE bulk orientational correlation time at this temperature would imply a value of approximately 1.1 for g_2. As discussed above, we might expect this parameter to increase in smaller pores, in which the liquid is likely to have a greater degree of order. However, a comparison of our values of $\langle\tau\rangle$ with those of Wallen et al. as a function of pore curvature suggests that g_2 decreases with decreasing pore size. In fact, the Raman average orientational correlation time becomes longer than the OKE average orientational correlation time for pore diameters on the order of 80 Å.

The source of the inconsistencies between the single-molecule reorientation data from NMR and Raman measurements and the collective reorientation data from our studies is not clear. One possibility is that additional OKE relaxation occurs on even longer time scales than studied here but that our apparatus is not sensitive enough to observe these dynamics. If this is the case, then the true values of $\langle\tau\rangle$ and $\langle\tau_{surf}\rangle$ reported would be larger than those reported here. On the other hand, the amplitude of any relaxation occurring on time scales longer than those observed here must be very small. Also, the fact that g_2 may be somewhat larger at the pore surfaces than in the bulk would tend to increase the average surface orientational time measured with OKE spectroscopy. This issue could be addressed by using an amplified laser system to further improve the dynamic range of the OKE data.

We have previously reported slow surface dynamics for a wetting liquid, acetonitrile, confined in porous glasses.[50] The decays for confined acetonitrile could be described by the sum of three exponentials, the middle of which was ascribed to the exchange of molecules from the pore surfaces into the bulk liquid.[50] Since we have fit the decays reported here to a sum of three exponentials as well, we should consider whether the intermediate exponential in the CS_2 decays arises from exchange. A number of lines of evidence suggest that this is not the case. First, the surface layer thickness for acetonitrile was at least one monolayer at all temperatures, as would be expected for a wetting liquid, whereas for CS_2 it is clear that not all molecules at the pore surfaces have inhibited dynamics. Second, upon surface modification, the dynamics of confined acetonitrile changed drastically, whereas the dynamics of confined CS_2 remain essentially identical. Finally, in acetonitrile, an Arrhenius plot of the time constant of the intermediate exponential revealed a lower activation energy than for reorientation in the bulk liquid, which is sensible if this exponential arises from exchange but not if it arises from reorientation. On the other hand, for CS_2 each surface exponential in each pore size has an activation energy that is as large or larger than that for the bulk liquid.

On the basis of the above three factors, we do not believe that exchange plays a role in the observed surface dynamics of CS_2. We also saw no signs of exchange in our previous study of methyl iodide,[41] which suggests that this not an important mechanism in the orientational diffusion of weakly wetting liquids in confinement. We believe that the crucial difference between the behavior of strongly wetting liquids and weakly wetting liquids lies in the nature of the inhibition of dynamics at the surface. In the case of strongly wetting liquids, all molecules at the pore surface have retarded dynamics due to strong solid/liquid interactions. For these molecules to exchange into the bulk, they must move some distance away from the surface. On the other hand, in the case of a weakly wetting liquid the inhibition of dynamics at the pore surfaces depends on the molecular orientation. Molecules that lie normal to the pore surfaces experience little or no retardation of orientational dynamics, while those that are flat on the surface experience the greatest retardation due to both geometrical and hydrodynamic volume effects. These latter molecules can "exchange" into the bulk liquid by rotating off of the surface, which means that for weakly wetting liquids the processes of exchange and reorientation are identical and therefore should not have separate signatures in the OKE decay.

V. Conclusions

The results presented here paint a detailed picture of the orientational dynamics of a weakly wetting liquid at silicate

glass surfaces. Despite the lack of strong interactions between liquid CS_2 and the pore surfaces, the data presented here demonstrate that in small enough pores a significant fraction of the surface orientational relaxation occurs on a time scale that is more than an order of magnitude slower than that in the bulk liquid. We have also shown that, by considering the dependence of the surface relaxation on the pore size, the different mechanisms that contribute to the retardation of orientational dynamics at the pore surfaces can be isolated. We have found in particular that the hydrodynamic volume for CS_2 reorientation increases by a factor of 2 at the pore surfaces. Most of the rest of the inhibition of reorientation at the pore surfaces can be accounted for by geometrical confinement effects, although interactions with the pore surfaces may play a small role as well. It remains possible that orientational dynamics occur in this system on time scales even longer than those reported here, which may help to reconcile our results with those of previous NMR[35] and Raman[38] studies. Performing further experiments at higher laser powers should help to address this question.

Acknowledgment. This work was supported by the National Science Foundation, Grant CHE-9501598. J.T.F. is a Research Corporation Cottrell Scholar and thanks the Camille and Henry Dreyfus Foundation for a New Faculty Award and the Alfred P. Sloan Foundation for a Sloan Research Fellowship.

References and Notes

(1) *Molecular Dynamics in Restricted Geometries*; Drake, J. M., Klafter, J., Eds.; Wiley: New York, 1989.
(2) *Dynamics in Small Confining Systems Extended Abstracts*; Drake, J. M., Klafter, J., Kopelman, R., Eds.; Materials Research Society: Pittsburgh, 1990; Vol. EA-22, p 248.
(3) *Dynamics in Small Confining Systems*; Drake, J. M., Klafter, J., Kopelman, R., Awschalom, D. D., Eds.; Materials Research Society: Pittsburgh, 1993; Vol. 290, p 377.
(4) *Dynamics in Small Confining Systems II*; Drake, J. M., Klafter, J., Kopelman, R., Troian, S. M., Eds.; Materials Research Society: Pittsburgh, 1995; Vol. 366, p 466.
(5) *Dynamics in Small Confining Systems III*; Drake, J. M., Klafter, J., Kopelman, R., Eds.; Materials Research Society: Pittsburgh, 1997; Vol. 464, p 388.
(6) Dijkstra, M. *J. Chem. Phys.* **1997**, *107*, 3277.
(7) Crassous, J.; Charlaix, E.; Loubet, J.-L. *Phys. Rev. Lett.* **1997**, *78*, 2425.
(8) Gupta, S. A.; Cochran, H. D.; Cummings, P. T. *J. Chem. Phys.* **1997**, *107*, 10316.
(9) Gupta, S. A.; Cochran, H. D.; Cummings, P. T. *J. Chem. Phys.* **1997**, *107*, 10327.
(10) Gupta, S. A.; Cochran, H. D.; Cummings, P. T. *J. Chem. Phys.* **1997**, *107*, 10335.
(11) Gao, J.; Luedtke, W. D.; Landman, U. *J. Chem. Phys.* **1997**, *106*, 4309.
(12) Gao, J.; Luedtke, W. D.; Landman, U. *J. Phys. Chem. B* **1997**, *101*, 4013.
(13) Gao, J.; Luedtke, W. D.; Landman, U. *Phys. Rev. Lett.* **1997**, *79*, 705.
(14) Gao, J.; Luedtke, W. D.; Landman, U. *J. Phys. Chem. B* **1998**, *102*, 5033.
(15) Christenson, H.; Gruen, D.; Horn, R.; Israelachvili, J. *J. Chem. Phys.* **1987**, *87*, 1834.
(16) Christenson, H. K.; Gruen, D. W. R.; Horn, R. G.; Israelachvili, J. N. *J. Chem. Phys.* **1987**, *87*, 1834.
(17) Israelachvili, J. N.; McGuiggan, P. M.; Homola, A. M. *Science* **1988**, *240*, 189.
(18) Israelachvilli, J. N.; McGuigan, P. M.; Homola, A. M. *Science* **1988**, *240*, 189.
(19) Israelachvili, J.; Kott, S.; Gee, M.; Witten, T. *Macromolecules* **1989**, *22*, 4247.
(20) Israelachvili, J. N.; Kott, S. J.; Gee, M. L.; Witten, T. A. *Macromolecules* **1989**, *22*, 4247.
(21) Hu, H.-W.; Carson, G. A.; Granick, S. *Phys. Rev. Lett.* **1991**, *66*, 2758.
(22) Hu, H.-W.; Carson, G. A.; Granick, S. *Phys. Rev. Lett.* **1991**, *66*, 2758.
(23) Homola, A. M.; Nguyen, H. V.; Hadziioannou, G. *J. Chem. Phys.* **1991**, *94*, 2346.
(24) Homola, A. M.; Nguyen, H. V.; Hadziioannou, G. *J. Chem. Phys.* **1991**, *94*, 2346.
(25) Granick, S. *Science* **1991**, *253*, 1374.
(26) Granick, S. *Science* **1991**, *253*, 1374.
(27) Brinker, C. J.; Scherer, G. W. *Sol−Gel Science: The Physics and Chemistry of Sol−Gel Processing*; Academic Press: San Diego, CA, 1990.
(28) Liu, G.; Mackowiak, M.; Jonas, J. *Chem. Phys.* **1990**, *149*, 165.
(29) Liu, G.; Mackowiak, M.; Li, Y.; Jonas, J. *J. Chem. Phys.* **1991**, *94*, 239.
(30) Liu, G.; Li, Y.; Jonas, J. *J. Chem. Phys.* **1991**, *95*, 6892.
(31) Koziol, P.; Nelson, S. D.; Jonas, J. *Chem. Phys. Lett.* **1993**, *201*, 383.
(32) Korb, J.-P.; Xu, S.; Jonas, J. *J. Chem. Phys.* **1993**, *98*, 2411.
(33) Korb, J.-P.; Delville, A.; Xu, S.; Demaulenaere, G.; Costa, P.; Jonas, J. *J. Chem. Phys.* **1994**, *101*, 7074.
(34) Xu, S.; Ballard, L.; Kim, Y. J.; Jonas, J. *J. Phys. Chem.* **1995**, *99*, 5787.
(35) Korb, J.-P.; Xu, S.; Cros, F.; Malier, L.; Jonas, J. *J. Chem. Phys.* **1997**, *107*, 4044.
(36) Lee, Y. T.; Wallen, S. L.; Jonas, J. *J. Phys. Chem.* **1992**, *96*, 7161.
(37) Yi, J.; Jonas, J. *J. Phys. Chem.* **1996**, *100*, 16789.
(38) Wallen, S. L.; Nikiel, L.; Jonas, J. *J. Phys. Chem.* **1995**, *99*, 15421.
(39) Warnock, J.; Awschalom, D. D.; Shafer, M. W. *Phys. Rev. B* **1986**, *34*, 475.
(40) Farrer, R. A.; Loughnane, B. J.; Fourkas, J. T. *J. Phys. Chem. A* **1997**, *101*, 4005.
(41) Loughnane, B. J.; Fourkas, J. T. *J. Phys. Chem. B* **1998**, *102*, 10288.
(42) Righini, R. *Science* **1993**, *262*, 1386.
(43) Gregg, S. J.; Sing, K. S. W. *Adsorption, Surface Area, and Porosity*; Academic Press: London, 1967.
(44) Iler, R. K. *The Chemistry of Silica*; Wiley: New York, 1979.
(45) Armistead, C. G.; Hockey, J. A. *Trans. Faraday Soc.* **1967**, *63*, 2549.
(46) Hair, M. L.; Hertl, W. *J. Phys. Chem.* **1969**, *73*, 2372.
(47) McMorrow, D.; Lotshaw, W. T. *J. Phys. Chem.* **1991**, *95*, 10395.
(48) Mukamel, S. *Principles of Nonlinear Optical Spectroscopy*; Oxford University Press: New York, 1995.
(49) Ladanyi, B. M.; Klein, S. *J. Chem. Phys.* **1996**, *105*, 1552.
(50) Loughnane, B. J.; Farrer, R. A.; Fourkas, J. T. *J. Phys. Chem. B* **1998**, *102*, 5409.
(51) Debye, P. *Polar Molecules*; Dover: New York, 1929.
(52) Kivelson, D.; Madden, P. A. *Annu. Rev. Phys. Chem.* **1980**, *31*, 523.
(53) Quintana, J.; Henderson, D.; Haymet, A. D. J. *J. Chem. Phys.* **1993**, *98*, 1486.
(54) Kierlik, E.; Rosinberg, M. L. *J. Chem. Phys.* **1994**, *100*, 1716.
(55) Padilla, P.; Toxvaerd, S. *J. Chem. Phys.* **1994**, *101*, 1490.
(56) Ma, W.-J.; Iyer, L. K.; Vishveshwara, S.; Koplik, J.; Banavar, J. R. *Phys. Rev. E* **1995**, *51*, 441.
(57) Murry, R. L.; Fourkas, J. T.; Keyes, T. *J. Chem. Phys.* **1998**, *109*, 2814.